Polymer growth mode on the heterogeneous Ziegler–Natta catalyst: active sites at the bottom of the growing polymer layer

Seong Han Kim and Gabor A. Somorjai *

Department of Chemistry, University of California at Berkeley and Materials Science Division, Lawrence Berkeley National Laboratory, Berkeley, CA 94720, USA

Received 14 May 2000; accepted 6 June 2000

By alternating the supply of propylene and ethylene monomers, alternating polypropylene and polyethylene films were produced on one model Ziegler–Natta catalyst. This way, we could show that the active polymerization sites remain under the growing polymer films and thus the monomer molecules must transport through the growing polymer to the active sites.

Keywords: Ziegler–Natta, model catalyst, active site, monomer diffusion, X-ray photoelectron spectroscopy, laser reflection interferometry

1. Introduction

Does a polymer chain grow out of an active site attached to the catalyst with monomer molecules being inserted at the bottom of the polymer chain? Or does the polymer chain detach the active site from the catalyst and grow by insertion of monomer molecules at the moving active site on top of the polymer chain? For high-surface-area heterogeneous Ziegler–Natta polymerization catalysts, the location of the active sites and the growth of polymer layer have been studied using mostly kinetics studies [1–8] and electron microscopic techniques [9–13]. The kinetics studies are an indirect approach where the average polymerization rates, measured under various reaction conditions, are fitted with a kinetic model based on reasonable assumptions. The electron microscopic techniques provide topographic images of polymer particles grown at an initial stage of polymerization and attempt to interpet the particle shapes in terms of polymer growth mode. But, these techniques require special sample treatments, such as chemical staining, conductive coating, or carbon replication, that may influence the topography of the nascent particles. In this paper we present a direct evidence that the polymer grows out of the active catalyst sites that remain anchored to the solid substrate.

Using laser reflection interferometry (LRI) and X-ray photoelectron spectroscopy (XPS), we monitored the polymerization of propylene and ethylene monomers that were reacted with a model catalyst film in sequence. The model catalyst film was fabricated by chemical vapor deposition of Mg and $TiCl_4$ on a flat Au substrate [14–17]. As propylene was introduced first into the reaction chamber, a thin film of polypropylene grew covering the catalyst surface. When ethylene was introduced second after the removal of the propylene monomer, the polyethylene grew underneath the polypropylene. Polymerization occurred by the diffusion of monomers through the growing polymer film. In addition, our model study proved that once the catalyst is activated with the triethylaluminum ($AlEt_3$) co-catalyst, aluminum-containing species are not involved in the polymerization process at the active sites and excess $AlEt_3$ is removed from the activated catalyst surface by the growing polymer molecules.

2. Experimental

The ultrahigh vacuum (UHV) chamber used in this study has been described in detail elsewhere [16]. Briefly, the apparatus consisted of a preparation chamber, an analysis chamber, and a polymerization reaction cell. The preparation chamber was equipped with an Ar ion sputter gun for sample cleaning, a magnesium source (Knudsen cell), an electron gun, and leak valves for gas introduction. The analysis chamber housed a PHI 5400 ESCA system for XPS measurement. The reaction cell was equipped with a temperature-controlled diode laser ($\lambda = 675$ nm) and a photodetector for *in situ* LRI measurements of polymer film growth. The model catalyst sample under study was transferred from one section of the apparatus to the others without exposure to air.

The $TiCl_x/MgCl_2$ model catalyst film was fabricated by co-deposition of $TiCl_4$ and Mg on an Au foil (1 cm^2) at 300 K in the preparation chamber. The details have been published elsewhere [14,15,17]. Its chemical composition was confirmed with XPS. Then, the $TiCl_x/MgCl_2$ model catalyst film was transferred into the reaction cell (heated to 340 K) and activated by exposure to 5 Torr of $AlEt_3$. Polymerization was carried with 900 Torr of ethylene or propylene.

* To whom correspondence should be addressed.

The polymer film growth on the model catalyst during polymerization was monitored with LRI [16]. The thickness of the polymer film at time t, $d_m(t_m)$, was calculated from the interference oscillation of the reflected laser beam using the following equation:

$$d_m(t_m) = \frac{m\lambda \cos\theta_1}{2n_1}, \quad (1)$$

where m is the number of periods of oscillation, $\lambda = 675$ nm, θ_1 is the laser beam propagation angle (10°) with respect to the surface normal, and n_1 is the refractive index of the polymer film. Given typical refractive indices of polyethylene and polypropylene of $n_1 = 1.50$–1.55 [18], one full cycle of oscillation between adjacent maximum corresponded to ∼222 nm.

The composition of the polymer films grown on the model catalyst film was measured with XPS. The X-ray source was Al K_α radiation (1486.6 eV). The pass energy of the XPS electron energy analyzer was 178.95 eV for a survey scan and 35.75 eV for a high-resolution scan. The C 1s peak (284.6 eV) was used as a reference for the energy scale.

3. Results and discussion

A priori, the polymer growth mode could be one or a combination of the following possibilities, depending on the location of the active sites during the polymerization:

(a) The active sites remain at the interface of the polymer and the catalyst phase and the polymer grows over the active sites [6–8]. Since the active sites are covered by the growing polymer layer, the polymer layer will act as a kinetic barrier for monomer transport to the active sites buried under the polymer layer.

(b) The active sites are separated from the catalyst surface and migrate to the interface of the polymer and the gas phase, and the polymer grows under the active sites. In this case, regardless of polymer thickness, there would be no kinetic barrier for monomer transport to the active sites [1,3].

(c) The catalyst phase undergoes significant fragmentation as polymerization occurs [9–13] and fresh active sites are newly produced available to the gas-phase monomer molecules.

In order to distinguish these possibilities, sequential polymerization of ethylene and propylene was carried out on a $TiCl_x/MgCl_2$ catalyst film deposited on an Au film and the surface composition of the polymer film was analyzed with valence-band XPS. If mode (a) were the case, the first-polymerized layer would be located on top of the second-polymerized layer. If mode (b) were the case, the first-polymerized layer would be found under the second-polymerized layer. If the catalyst phase fragments as in mode (c), the surface composition of the sequentially polymerized film would have both polymer components depending on the degree of the catalyst fragmentation. The mixed surface composition of two polymers can also originate from a dynamic operation of both mode (a) and mode (b). The following paragraphs describe our experimental observations supporting mode (a) only.

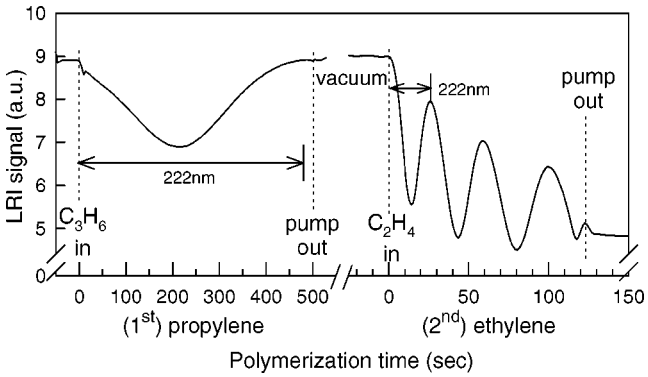

Figure 1. Polymer film growth monitored with LRI during sequential polymerization of propylene and ethylene on a $TiCl_x/MgCl_2$ catalyst film (note the change in the time scale). The model catalyst was activated by exposure to 5 Torr of $AlEt_3$. Polymerization was performed without the $AlEt_3$ co-catalyst in the gas phase. The monomer pressure was 900 Torr for both propylene and ethylene. The polymerization temperature was 340 K. The thicknesses of polypropylene and polyethylene, calculated from the LRI data, were ∼230 and ∼780 nm, respectively.

Thin layers of polypropylene (PP) and polyethylene (PE) were sequentially grown on a $TiCl_x/MgCl_2$ catalyst film. Figure 1 shows the LRI signal changes as a function of time during the sequential polymerization of (1) ∼230 nm thick PP film and (2) ∼780 nm thick PE film on the catalyst film pre-activated with $AlEt_3$. The monomer pressures were 900 Torr in both polymerization processes and no $AlEt_3$ was present in the gas phase. At the first maximum of the LRI signal corresponding to ∼222 nm thick PP film, the LRI signal intensity of the polymer-covered catalyst was almost the same as that of the catalyst film prior to exposure to propylene. This implied that the PP film surface was very smooth and there was no (or negligible) fragmentation of the catalyst film [16], ruling out mode (c). When propylene was pumped out, the polymerization process stopped immediately. Upon introduction of ethylene, the polymerization resumed immediately. A shorter periodicity in the LRI signal oscillation resulted from a faster polymerization rate of ethylene, compared to propylene [16].

In figure 2, the valence-band XPS of the sequentially polymerized film (PP first then PE second, figure 1) is compared with those of pure PP and PE films grown separately. The PE film had two C 2s peaks at ∼14 and 18.3 eV that corresponded to the antibonding and bonding orbitals of the carbon in the $–CH_2–$ backbone, respectively [19,20]. The PP film had an additional C 2s peak at 16 eV of the carbon in the $–CH_3$ group. In the case of the sequentially polymerized film, the C 2s spectrum showed three peaks characteristic of the PP film and no contribution from the

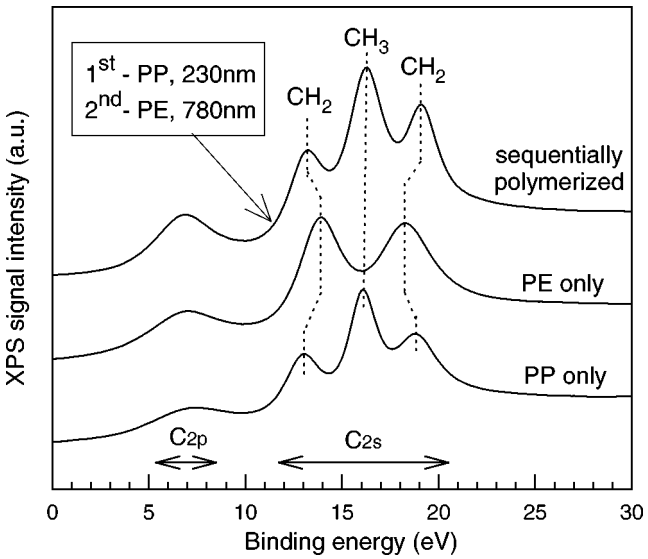

Figure 2. Valence band XPS spectrum of the sequentially grown polymer film (figure 1) and comparison with those of pure polyethylene and polypropylene films grown separately. The peaks at ∼13 and ∼19 eV result from the C 2s antibonding and bonding orbitals of $-CH_2-$ in the polymer backbone, respectively. The peak at 16 eV comes from the C 2s orbital of the CH_3 group. The photoelectrons from the C 2p orbitals appear at around 7 eV. (Pass energy of XPS measurements = 35.75 eV.)

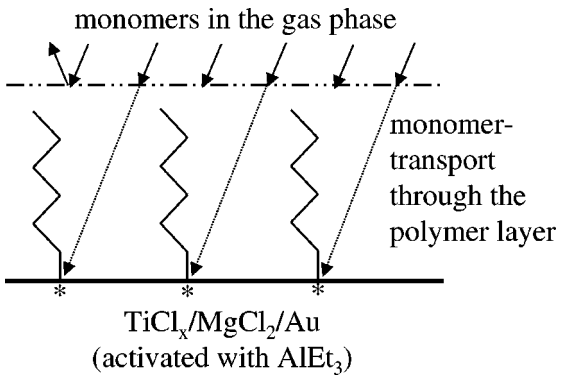

Scheme 1.

PE film. This result indicated that the first-polymerized PP layer was at the film surface and the second-polymerized PE layer was under the PP layer. Therefore, it could be concluded that mode (a) is the case, i.e., the active sites for polymerization remain at the polymer/substrate interface. Scheme 1 illustrates mode (a) where the active sites are present at the bottom of the growing polymer layer and the monomer molecules are transported through the polymer layer to the active sites.

In a separate experiment, a PE film of ∼10 μm thickness was grown on a $TiCl_x/MgCl_2$ model catalyst in the presence of excess $AlEt_3$ (5 Torr) in the gas phase. After polymerization, the PE film was peeled off from the Au substrate in air, placed into the UHV chamber, and analyzed with XPS. Figure 3 represents the survey spectra of the top and bottom of the peeled-off film. The catalyst components (Mg, Ti, and Cl) were detected only in the bottom spectrum. This result also supported mode (a) where the active

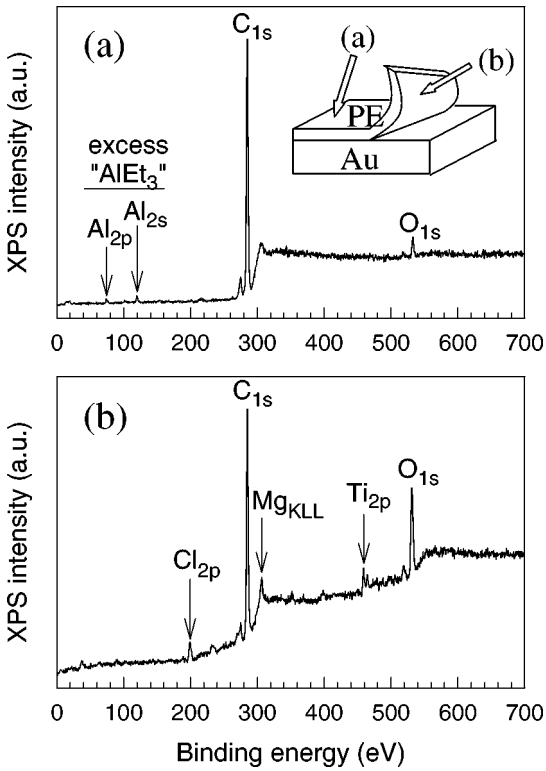

Figure 3. XPS of the (a) top and (b) bottom of the peeled-off polyethylene film grown on a $TiCl_x/MgCl_2$ catalyst film. The thickness of the polyethylene film was ∼10 μm and the film was peeled off in air. Polymerization was performed with 900 Torr of ethylene in the presence of 5 Torr of $AlEt_3$ in the gas phase. The catalyst temperature was 340 K. (Pass energy of XPS measurement = 178.95 eV.)

sites remain at the polymer/substrate interface during the polymerization on the $TiCl_x/MgCl_2$ film.

It also should be noted in figure 3 that the Al 2s and 2p peaks were not detected at the bottom spectrum of the polymer, while they were observable in the top spectrum due to the presence of excess $AlEt_3$ in the gas phase. This implied that the aluminum-containing species, by-products of the catalyst activation by $AlEt_3$, are not attached to the activated catalyst surface and removed by the growing polymer molecules, ruling out a bimetallic active site model [2,21]. Furthermore, this result indicated that once the polymer film covers the catalyst surface, there is no additional effect of excess $AlEt_3$ on the polymerization kinetics of the active sites under the polymer film.

An additional supporting evidence for monomer diffusion through the polymer film, as in mode (a), was observed in the LRI experiments. Figure 4 reports the LRI signal changes due to the presence of the gas-phase molecules over a polypropylene film (∼650 nm thick) at 70 °C. When propylene (monomer) was filled in the reaction cell, the LRI intensity increased nonlinearly over time (figure 4 (left side)). When propylene was pumped out from the cell, the signal decreased slowly in a nonlinear manner. This behavior was in contrast to the insensitivity of the LRI intensity to the presence of an inert gas (argon) shown in figure 4 (right side). The effect of propylene on the LRI intensity

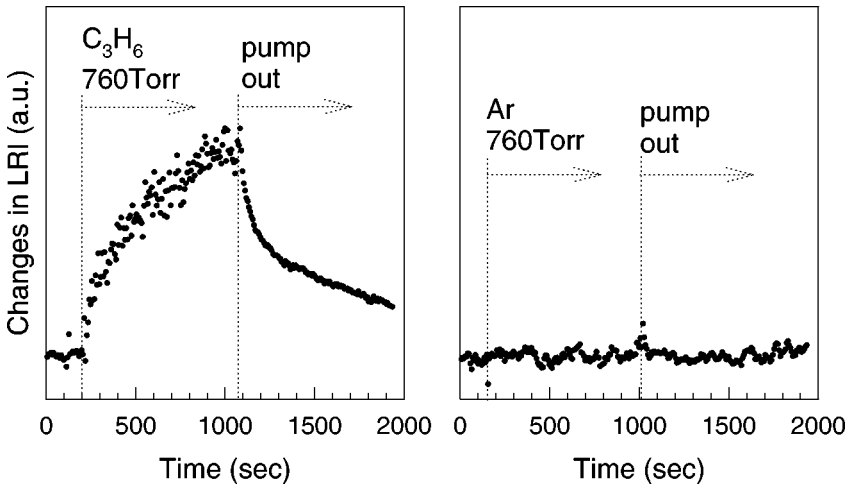

Figure 4. Changes in the LRI signal due to the presence of C_3H_6 (left side) and Ar (right side) in the gas phase over a propylene film (thickness = 650 nm). Note that a slight shift in the base line due to the gas-phase refractive index change has been subtracted. The polymer and gas temperature was 340 K.

could be attributed to the high solubility and slow diffusion rate of the monomer gas in the polymer [22,23]. As the monomer gas dissolved and diffused into the polymer film, the polymer film swelled accordingly, changing its refractive index (n_1) as well as its thickness (d). Upon pumping, the monomer molecules dissolved in the polymer desorbed slowly into the vacuum, the desorption rate being limited by the monomer diffusion rate in the polymer. By contrast, the presence of argon in the gas phase changed neither the polymer refractive index nor the film thickness because its solubility in the polymer was negligible.

Active site encapsulation and monomer diffusion in the growing polymer layer will play an important role in catalyst deactivation kinetics. It is a well known phenomenon that the polymerization activity of the supported Ziegler–Natta catalyst decreases as the polymerization continues. In many cases, the decay of the polymerization rate has been explained with simple kinetic models such as first-order decay processes of two different active sites [24,25], bimolecular decay processes via coupling of two adjacent sites [2,26], destructive reactions of the active sites with excess $AlEt_3$ [27]. However, scheme 1 rejects these simple models that consider only chemical aspects of the alteration of active sites and not the physical aspects of the monomer transport trough the polymer layer. As the polymer film grows thicker, the diffusion barrier for monomer transport to the active sites will increase, lowering the polymerization rate. It should also be noted that the morphology of the polymer film changes in a complex way as polymerization proceeds [10–13,16], affecting the monomer transport kinetics. These changes in the polymer thickness and morphology should be considered in kinetic modeling and theoretical simulations of polymerization processes [6–8] in order to understand the nature of deactivation in the heterogeneous Ziegler–Natta polymerization system.

It is also known for the heterogeneous Ziegler–Natta catalysts that co-polymerization of ethylene with α-olefins increases the polymerization rate for ethylene, compared to ethylene homo-polymerization [23,28]. This enhancement effect of the ethylene polymerization rate can be explained by the monomer transport through the growing polymer as in scheme 1. When ethylene is co-polymerized with α-olefins, the growing polymer layer covering the active sites will contain more amorphous phase. Compared to the pure polyethylene layers containing more crystalline phase, the amorphous phase in the co-polymer layer will permit enhanced monomer transport to the active sites [22], enhancing the concentration of monomers available for polymerization at the active sites under the growing polymer layer.

4. Conclusions

The location and composition of the active sites during the polymerization were experimentally proved by utilization of a $TiCl_x/MgCl_2$ catalyst film and *in situ* analysis of the polymer film, produced on it, using laser reflection interferometry and X-ray photoelectron spectrometry. The active sites were always present at the interface of the catalyst and the growing polymer and polymerization at the active sites occurred by the diffusion of monomers through the growing polymer layer. The aluminum-containing products from the catalyst activation reaction with $AlEt_3$ were not involved in the polymerization process at the active sites and these species, as well as excess $AlEt_3$, were removed from the active sites by the growing polymer molecules.

Acknowledgement

This work was supported by the Director, Office of Energy Research, Office of Basic Energy Sciences, Material Science Division, of the US Department of Energy under Contract No. DE-AC03-76SF00098. The authors also acknowledge support from Montell USA, Inc.

References

[1] L.L. Böhm, Polymer 19 (1978) 545.
[2] T. Keii, E. Suzuki, M. Tamura, M. Murata and Y. Doi, Makromol. Chem. 183 (1982) 2285.
[3] R. Spitz, J.L. Lacombe and A. Guyot, J. Polym. Sci. Polym. Chem. Ed. 22 (1984) 2625.
[4] G. Galvin and M. Tirrell, Chem. Eng. Sci. 41 (1986) 2385.
[5] S. Floyd, T. Heiskanen, T.W. Taylor, G.E. Mann and W.H. Ray, J. Appl. Polym. Sci. 33 (1987) 1021.
[6] T.F. Mckenna, J. Dupuy and R. Spitz, J. Appl. Polym. Sci. 57 (1995) 371.
[7] M. Hamba, G.C. Han-Adebekun and W.H. Ray, J. Polym. Sci. Polym. Chem. Ed. 35 (1997) 2075.
[8] A. Shariati, C.C. Hsu and D.W. Bacon, Polym. Reac. Eng. 7 (1999) 97.
[9] J.Y. Gutman and J.E. Guillet, Macromolecules 3 (1970) 470.
[10] M. Kakugo, H. Sadatoshi, M. Yokoyama and K. Kojima, Macromolecules 22 (1989) 547.
[11] M. Kakugo, H. Sadatoshi, J. Sakai and M. Yokoyama, Macromolecules 22 (1989) 22.
[12] L.C. Santa Maria, F.M. Coutinho and J.C. Bruno, Eur. Polym. J. 29 (1993) 1319.
[13] L. Noristi, E. Marchetti, G. Baruzzi and P. Sgarzi, J. Polym. Sci. A 32 (1994) 3047.
[14] S.H. Kim and G.A. Somorjai, J. Phys. Chem. B 104 (2000), in issue of 29 June.
[15] S.H. Kim and G.A. Somorjai, Appl. Surf. Sci., in press.
[16] S.H. Kim, G. Vurens and G.A. Somorjai, J. Catal., in press.
[17] S.H. Kim, C.R. Tewell and G.A. Somorjai, Langmuir, submitted.
[18] V. Galiatsatos, R.O. Neaffer, S. Sen and B.J. Sherman, in: *Physical Properties of Polymers Handbook*, ed. J.E. Mark (American Institute of Physics, New York, 1996) p. 535.
[19] T. Gross, A. Lippitz, W.E.S. Unger, J. Friedrich and C. Woll, Polymer 35 (1994) 5901.
[20] J. Delhalle, J. Riga, J.P. Denis, M. Deleuze and M. Dosiere, Chem. Phys. Lett. 210 (1993) 21.
[21] K. Kohara, M. Shinogama, Y. Doi and T. Keii, Makromol. Chem. 180 (1979) 2139.
[22] S.A. Stern, B.M. Krishnakumar and S.M. Nadakatti, in: *Physical Properties of Polymers Handbook*, ed. J.E. Mark (American Institute of Physics, New York, 1996) ch. 50.
[23] N.M. Gultseva, T.M. Ushakova, A.M. Aladyshev, L.N. Raspopov and I.N. Meshkova, Polym. Bull. 29 (1992) 639.
[24] P.J.T. Tait and S. Wang, Polym. J. 20 (1988) 499.
[25] P. Galli, L. Luciani and G. Cecchin, Angew. Makromol. Chem. 94 (1981) 63.
[26] J.C.W. Chien and C. Kuo, J. Polym. Sci. Polym. Chem. Ed. 24 (1986) 2707.
[27] P. Pino, B. Rotzinger and E. von Achenbach, Makromol. Chem. Suppl. 13 (1985) 105.
[28] J. Kovumaki and J.V. Seppala, Macromolecules 26 (1993) 5535.